Volume 282
Number 5
9 October 1998

JMB

JOURNAL OF MOLECULAR BIOLOGY

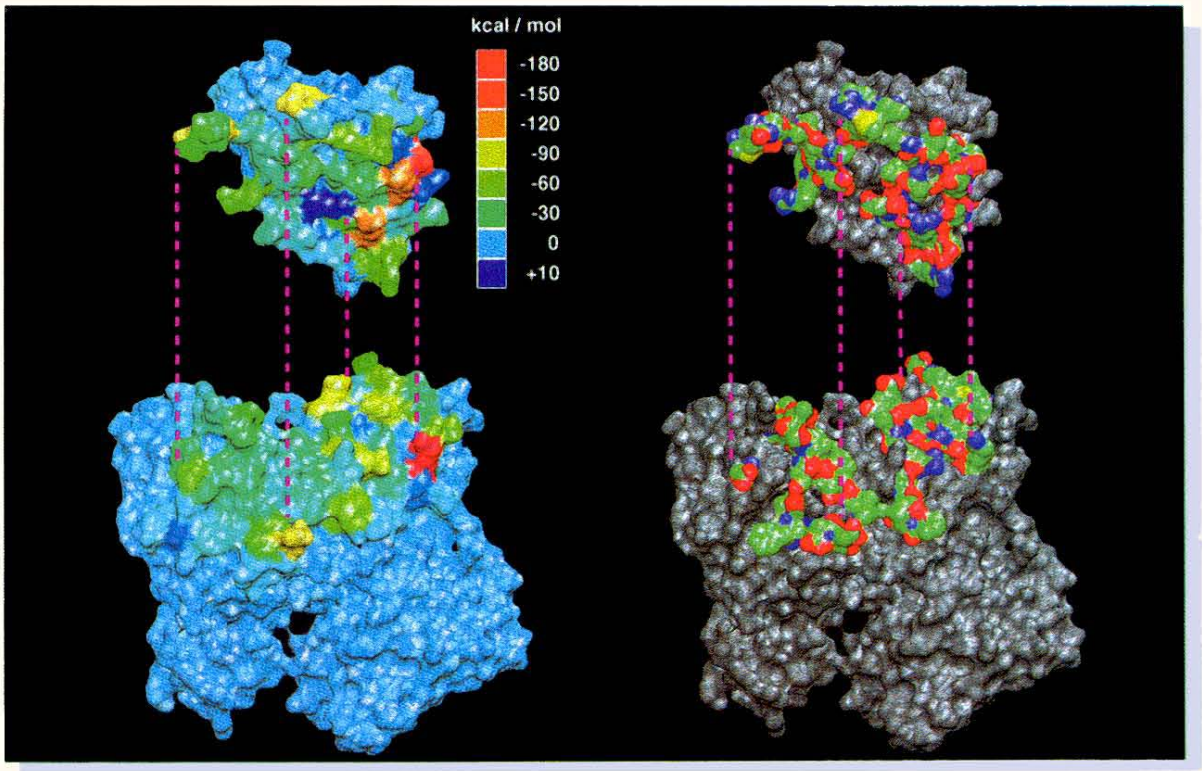

ACADEMIC PRESS
282 (5) 921–1094 ISSN 0022–2836
0022-2836(199810)282:5;1-P

Article No. mb982048 *J. Mol. Biol.* (1998) **282**, 921–932

JMB

COMMUNICATION

Cofilin and Gelsolin Segment-1: Molecular Dynamics Simulation and Biochemical Analysis Predict a Similar Actin Binding Mode

Willy Wriggers[1]*, Jay X. Tang[2], Toshifumi Azuma[2], Peter W. Marks[2] and Paul A. Janmey[2]

[1]*Department of Chemistry and Biochemistry, University of California, San Diego 9500 Gilman Drive, La Jolla CA 92093-0365, USA*

[2]*Brigham and Women's Hospital, Harvard Medical School, 221 Longwood Avenue Boston, MA 02115, USA*

**Corresponding author*

An understanding of the actin-depolymerizing function attributed to members of the ADF/cofilin/destrin superfamily requires a structural model of these proteins in complex with actin. As a step toward defining actin-cofilin interactions, the complex of yeast cofilin with monomeric actin was predicted, starting with the actin-gelsolin segment-1 binding mode recently suggested for the actin-destrin complex. After refinement by molecular dynamics simulation, the structure of cofilin converged in a new binding mode that required only minimal changes induced in the actin-cofilin interface. The predicted complex exhibits strong interactions between the N termini of actin and cofilin, mediated by a salt bridge of cofilin Arg3 with actin Asp1. The forming of this salt bridge could be prevented by the phosphorylation of cofilin Ser4, which is believed to inhibit cofilin depolymerization activity. Recent mutagenesis studies, crosslinking experiments and peptide binding studies are consistent with the predicted model of the actin-cofilin complex. The structural homology between cofilin and gelsolin segment-1 binding to actin was confirmed experimentally by two types of competitive binding assays.

Keywords: cofilin; gelsolin; ADF, destrin; actin binding site; molecular dynamics

The ADF/cofilin family of proteins, which includes destrin, depactin, and actophorin, are potent regulators of actin assembly in mammalian tissues and other cell types. For example, overexpression of cofilin in *Dictyostelium* cells induces membrane ruffling and cell motility (Aizawa *et al*., 1996), whereas microinjection of labeled cofilin in cultured muscle cells disrupts cytoplasmic F-actin and promotes formation of nuclear rods containing both actin and cofilin (Nagaoka *et al*., 1995). Nuclear rod formation is a common response of several cell types to heat or chemical stresses (Nishida *et al*., 1987; Yahara *et al*., 1996). The complex activity of cofilin *in vivo* can be inferred from the number of different reactions between cofilin/ADF and actin *in vitro*. Depending on such factors as pH, the presence of inositol phospholipids, the phosphorylation state of cofilin, the type of nucleotide bound to actin, and the presence of competing actin ligands, including heavy meromyosin, tropomyosin, caldesmon and phalloidin (Yonezawa *et al*., 1988), cofilin can bind actin monomers (G-actin) and filaments (F-actin), bundle actin filaments, disassemble F-actin, and inhibit nucleotide exchange from G-actin (reviewed by Moon *et al*., 1993). The binding of cofilin to F-actin also induces a change in the helical pitch of the filaments not yet observed with any other actin binding protein (McGough *et al*., 1997). The rapid disassembly of F-actin by cofilin has been interpreted variously as evidence for filament severing activity (Mabuchi, 1983; Maciver *et al*., 1991; Nishida *et al*., 1985) or acceleration of monomer disassembly at the pointed end of the actin filament (Carlier *et al*., 1997).

To elucidate the function of cofilin and related proteins, several studies have sought to define the cofilin/actin binding interface by chemical (Sutoh & Mabuchi, 1986), crystallographic (Leonard *et al*., 1997), and NMR methods (Hatanaka *et al*., 1996).

Abbreviations used: MD, molecular dynamics.

E-mail address of the corresponding author: wriggers@ucsd.edu

0022–2836/98/400921–12 $30.00/0

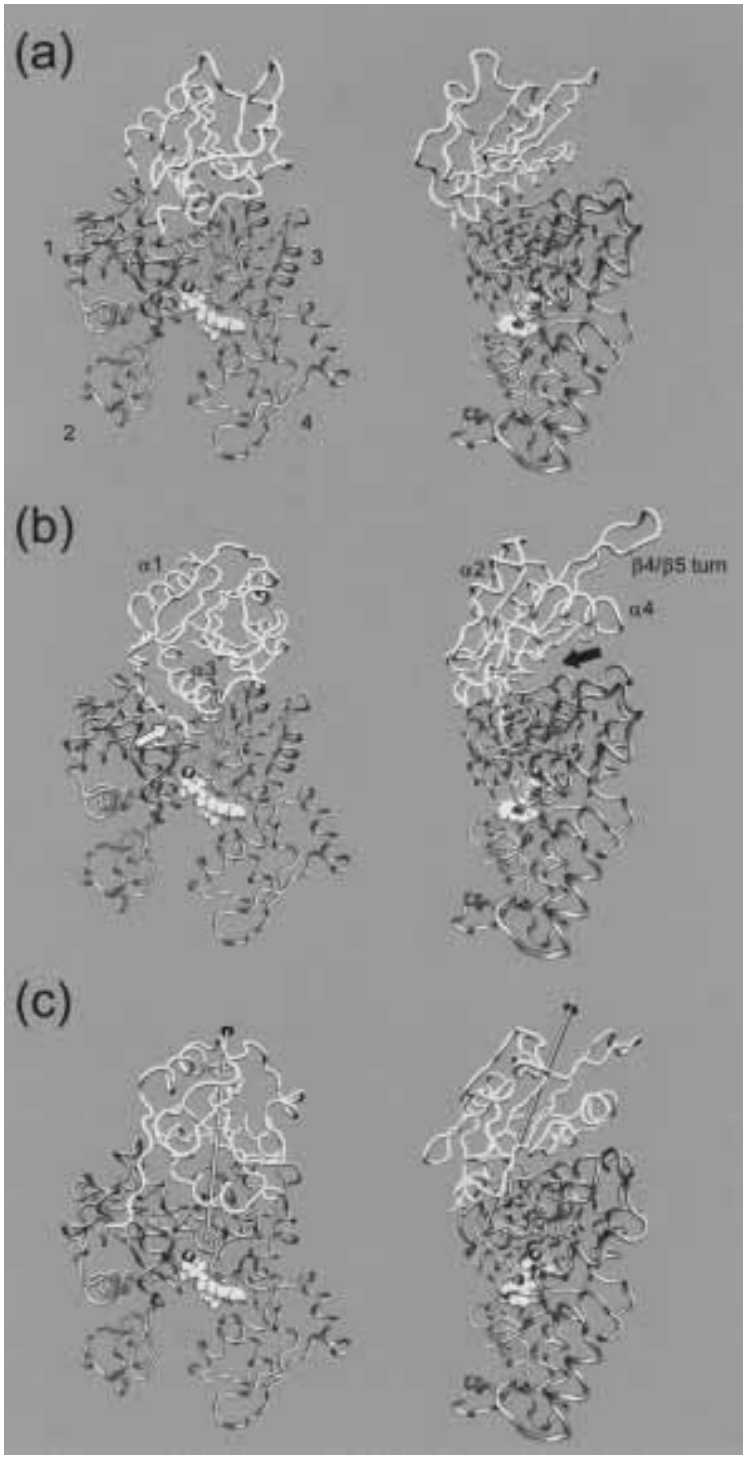

Figure 1. (a) Crystal structure of the actin-gelsolin segment-1 complex from McLaughlin *et al*. (1993). Left: front view; right: side view. Gelsolin segment-1 is shown in white tube representation, actin in grey tube representation. ATP (light gray) and the associated Ca ion (dark gray) are represented by van-der-Waals spheres. The numbers identify actin's structural subdomains (Kabsch *et al*., 1990). The coordinates of the actin-gelsolin segment-1 complex (McLaughlin *et al*., 1993) were supplied by Paul McLaughlin. The molecules in Figures 1 to 3 were rendered with the program VMD (Humphrey *et al*., 1996). (b) Cofilin crystal structure with added C and N termini aligned to actin in the suggested gelsolin segment-1 binding mode (Hatanaka *et al*., 1996). Left: front view; right: side view. Cofilin is shown in white tube representation, actin in grey tube representation. ATP (light gray) and the associated calcium ion (dark gray) are represented by van-der-Waals spheres. The white arrow marks a steric clash of the cofilin N terminus with actin. The black arrow points to a cleft between the two proteins. Prominent secondary structure elements of cofilin (Fedorov *et al*., 1997) are identified. The coordinates of cofilin residues 6 to 140, including 32 crystal water molecules (Fedorov *et al*., 1997) and of destrin (Hatanaka *et al*., 1996) were provided by Steven Almo and Hideki Hatanaka. (c) Predicted actin-cofilin complex. Left: front view; right: side view. Cofilin is shown in white tube representation, actin in grey tube representation. Actin's subdomains 2 and 4 were added back to the system after simulation. ATP (light gray) and the associated calcium ion (dark gray) are represented by van-der-Waals spheres. For the simulation of cofilin, residues 1 to 5 and 141 to 143, which are missing in the cofilin crystal structure (Fedorov *et al*., 1997), were added with the molecular modeling program Quanta (Molecular Simulations Inc., 1994). The cofilin-actin complex was built from the model of the destrin-actin complex, exploiting the homology of cofilin with destrin. As described by Hatanaka *et al*. (1996), 68 residues of destrin were superimposed by the corresponding residues of gelsolin segment-1. Cofilin was then superimposed by the 81 conserved residues of destrin which were identified by sequence alignment (Moon *et al*., 1993). To reduce the system size for simulation of the actin-cofilin complex, actin's subdomains 2 (residues 33 to 78) and 4 (residues 179 to 273), the actin-bound ATP nucleotide, and all actin or gelsolin-associated calcium ions (McLaughlin *et al*., 1993) were deleted. The interaction between rigid actin and cofilin fragments was optimized *in vacuo* by rigid-body energy minimization with the program X-PLOR (Brünger, 1992), followed by refinement in aqueous solution. The biopolymers were immersed in a shell of explicit water molecules of 5 Å thickness, which corresponds to approximately two layers of water molecules. Water molecules overlapping with the protein structures and

Such studies reveal that the cofilin N-terminus, which contains a critical phosphorylation site (Morgan *et al*., 1993; Nebl *et al*., 1996; Ohta *et al*., 1989) at Ser4 (yeast cofilin numbering) interacts with actin, as do peptides derived from cofilin's C terminus (Moriyama *et al*., 1992; Van Troys *et al*., 1997; Yonezawa *et al*., 1989). Similarly, both the N and C-terminal regions of actin can be linked to ADF (Sutoh & Mabuchi, 1986). A structural interpretation of the available biochemical data based on a destrin structure obtained by NMR (Hatanaka *et al*., 1996) suggests a mode of binding to G-actin that is very similar to that of the complex of actin with gelsolin segment-1, determined by X-ray crystallography (McLaughlin *et al*., 1993).

The present study was designed to test the hypothesis that cofilin binding to G-actin is structurally analogous to the complex formed between gelsolin segment-1 and subdomains 1 and 3 of the actin monomer (Figure 1(a)). To this end, molecular dynamics (MD) calculations were used to evaluate the quality of a cofilin-actin binding interface analogous to that of the gelsolin segment-1-actin contact. The usefulness of MD in molecular docking was recently demonstrated in the prediction of a complex between the chromosomal protein HMG-D and DNA (Balaeff *et al*., 1998). Computer algorithms for the prediction of protein aggregation modes have been developed in several laboratories, but the predictions are still far from routine (Strynadka *et al*., 1996). Compared to *ab initio* algorithms that perform a search for suitable candidate structures by rigid-body transformations, MD simulations provide a less exhaustive sampling of possible binding conformations. However, in this work other biochemical and structural data were available to assist in the molecular docking.

One essential requirement for the proper complex formation is the conformational flexibility of the binding interface, as provided by MD. The possible actin binding mode appears to depend, in particular, on the conformation of cofilin's functionally relevant N terminus, since the equivalent region in destrin exhibits steric clashes with actin in the gelsolin segment-1 binding mode (Hatanaka *et al*., 1996). The five N-terminal residues were not defined in the cofilin crystal (Fedorov *et al*., 1997) and had to be added in this work by modeling.

Computational models of protein aggregates are often of limited practical value unless they are substantiated by experimental measurements. Here we have adopted a hybrid simulation/biochemical approach. In conjunction with the modeling effort, two types of biochemical assays examine the extent to which cofilin and gelsolin compete for binding to actin monomers. The actin-binding behavior of both intact gelsolin and the truncated form GS160 (gelsolin residues 26 to 160) was studied. GS160 comprises the complete cytoplasmic gelsolin segment-1. This construct is ten residues larger than the N-terminal domain prepared by proteolytic digestion of gelsolin (resisues 1 to 149) and crystallized in complex with actin, but appears as a single folded domain in the whole gelsolin structure. In contrast to the N-terminal domain (residues 1 to 149) which binds only actin monomers, GS160 also interacts with F-actin to accelerate actin depolymerization, and so may be a closer analog of cofilin.

Modeling and molecular dynamics

To obtain a starting structure for the prediction of the complex we aligned the yeast cofilin crystal structure to actin in the gelsolin segment-1 binding mode (Hatanaka *et al*., 1996) and added cofilin's C and N termini. The resulting complex is shown in Figure 1(b) and compared to the structure of the gelsolin segment-1-actin complex in Figure 1(a). Similar to the model of the actin-destrin complex (Hatanaka *et al*., 1996), this alignment produced steric clashes of cofilin's N terminus with actin. To alleviate unfavorable interactions at cofilin's N terminus, residues 1 to 8 were temporarily removed from the protein, and cofilin's coordinates (including the 32 crystal water molecules) were shifted by 1 Å in the direction normal to the initial actin binding face. Compared to gelsolin segment-1 (Figure 1(a)), cofilin's structural elements extend further away from actin, giving rise to reduced contact in this binding mode (Figure 1(b)). To strengthen the binding interface, the complex was rigid-body energy minimized, solvated, and refined in a simulated annealing protocol of 170 ps duration (Wriggers & Schulten, 1998).

Inability to identify cofilin's residues 1 to 5 in the crystal suggests a high flexibility of the N terminus, leading to spatial disorder (Fedorov *et al*., 1997). Secondary structure prediction, using the Holley/Karplus (Holley & Karplus, 1989) and GOR (Garnier *et al*., 1978) methods implemented in the program Quanta (Molecular Simulations Inc., Burlington, Massachusetts) indicates a random coil state of cofilin's eight N-terminal residues (data not shown). After the first annealing run, the protein

non-crystallographic water molecules at the interface of actin and cofilin were removed. After solvation, the total system size was 9004 atoms (1087 water molecules). The system was subsequently refined by simulated annealing. We chose simulation protocols of 170 ps length with a maximum temperature of 500 K. Protocols and molecular dynamics parameters are described in detail elsewhere (Wriggers & Schulten, 1998). We characterized the movements of cofilin relative to the gelsolin segment-1 binding mode (b) by the classical screw axis of rigid-body movement (Chasles, 1830; Goldstein, 1980; Babcock *et al*., 1994). This axis identifies the relative movement of proteins or of protein domains that can be considered rigid. The rotation about the axis is right-handed (31°) and the direction and magnitude of the translation are indicated by the direction and length (1.8 Å) of the cone-shaped pointer.

had shifted relative to actin so that it was possible to add the N terminus back to the protein by exploiting its flexibility in the coil state: The predicted conformation of the N-terminal chain was sterically constrained by nearby actin and cofilin residues. Moreover, it was possible to secure an electrostatic complementary of the actin-cofilin interface by forming a salt bridge between cofilin Arg3 and the adjacent actin Asp1. After re-solvation, the system was refined in a second annealing run.

Two basic residues of cofilin (Arg96 and Lys98) are involved in actin binding (Lappalainen *et al.*, 1997; Moriyama *et al.*, 1992; Yonezawa *et al.*, 1991a,b). After the second annealing run, Arg96 and Lys98 were found within hydrogen bonding distance of two corresponding acidic residues of actin (Asp25 and Glu334, respectively). The side-chains of Arg96 and Lys98 were re-oriented to form salt bridges with the corresponding acidic residues of actin. The re-solvated complex was finally refined in a third simulated annealing run of 170 ps duration.

The predicted structure of the actin-cofilin complex is shown in Figure 1(c). The structure of cofilin converged in a new orientation relative to actin. Cofilin's movement relative to the gelsolin segment-1 binding mode (Figure 1(b)) can be characterized by least-squares fitting (Kabsch, 1976) as a right-handed rotation of 31° about the shown screw axis and by a short translation of 1.8 Å along the axis (helical rise).

Complex interface

The non-bonded energies arising in the complex allow one to identify the interacting residues when mapped to the protein surface (Figure 2(a)). About 20 residues from each protein form hydrogen bonds between the proteins. Most of the hydrogen bonds correspond to salt bridges between residues of opposite electrostatic charge. The interaction energies are predominantly attractive, in some cases involving values of −100 kcal/mol. A detailed analysis revealed that the Lennard-Jones contributions to the interaction energies (equation (1), Figure 2(a)) did not exceed 10 kcal/mol per residue, i.e. the interaction energies in equation (1) are mostly of electrostatic origin.

Figure 2(a) demonstrates that the actin-cofilin interface is surrounded by a rim of polar residues involved in salt bridges. Specifically, the side-chains of actin's Asp1, Asp25, Glu334, Arg147, Lys328, Asp292/Glu167, and Asp288 interact with cofilin's corresponding side-chains Arg3, Arg96, Lys98, Asp91, Glu126/Asp123, Arg135, and Arg138. A single residue, cofilin's Asp118, exhibits a slightly repulsive interaction enthalpy with actin (+9.6 kcal/mol), due to its close (6 Å) proximity to actin's acidic cluster Asp292/Glu167/Thr148. The negative charge of this solvent-exposed side-chain is expected to be screened by the surrounding dielectric and by counterions.

We note that the high interaction energies in Figure 2(a), which are of the same order of magnitude as molar lattice energies of salt crystals (Israelachvili, 1992), would arise in a medium of dielectric permitivity $\varepsilon = 1$ (e.g. *in vacuo*). Actual electrostatic interaction energies can be expected to be considerably lower, as they scale with the inverse dielectric permitivity of the protein/solvent environment (Israelachvili, 1992): MD simulations have suggested values for the protein dielectric permitivity ranging from 10 to 36 (King *et al.*, 1991; Smith *et al.*, 1993); bulk water at room temperature has a value $\varepsilon = 80$. Dielectric screening, hydration energies and significant entropic contributions in solvated proteins lower the effective free energies to values of about 5 kcal/mol (Anderson *et al.*, 1990) per salt bridge formed. These effects are present in the simulation by means of the explicit solvent and the conformational variability of the evolving system.

Alanine scanning mutagenesis of the interface between human growth hormone and the extracellular domain of its first bound receptor demonstrated that the interface resembles a cross-section through a globular protein, where a small, central hydrophobic core region is surrounded by hydrophilic residues (Clackson & Wells, 1995). It was argued that this property may be general to protein-protein interfaces. An inspection of the buried contact surface of the actin-cofilin complex (Figure 2(b)) reveals a central apolar cluster formed by actin's residues Ile341 and Ile345, and by cofilin's residues Met99, Tyr101, and Ala102. This apolar cluster is part of cofilin's actin-binding helix 3 (residues 95 to 111). The core contact surface also includes Ser103, which exhibits only weak enthalpic interactions with actin (Figure 2(b)). The corresponding contact surface of actin is formed by Ile341 and Ile345, and by Ser344 and Ser348. The buried surface area of the actin-cofilin interface (Figure 2(b)) measures 1390 Å^2, and is about twice as large as the buried area of the actin-gelsolin segment-1 interface (640 Å^2; Figure 1(a)). This increase in contact surface can be attributed to both the described interactions of cofilin's N-terminal residues 1 to 8 with actin (330 Å^2) and to the closure of the cleft present in the Hatanaka model of the complex (Figure 1(b)).

Induced conformational changes

To analyze the convergence and stability of the system we compared the individual protein deviations with the temperature of the system in the three simulated annealing runs (data not shown). The system followed closely the annealing target temperature and the rate of conformational change was enhanced by high temperatures (300 to 500 K) which facilitate the crossing of potential energy barriers. Initially, cofilin's structure remained close to the crystal conformation (1.5 Å rms deviation after the first annealing run). The addition of the cofilin N-terminal residues 1 to 8 had little effect

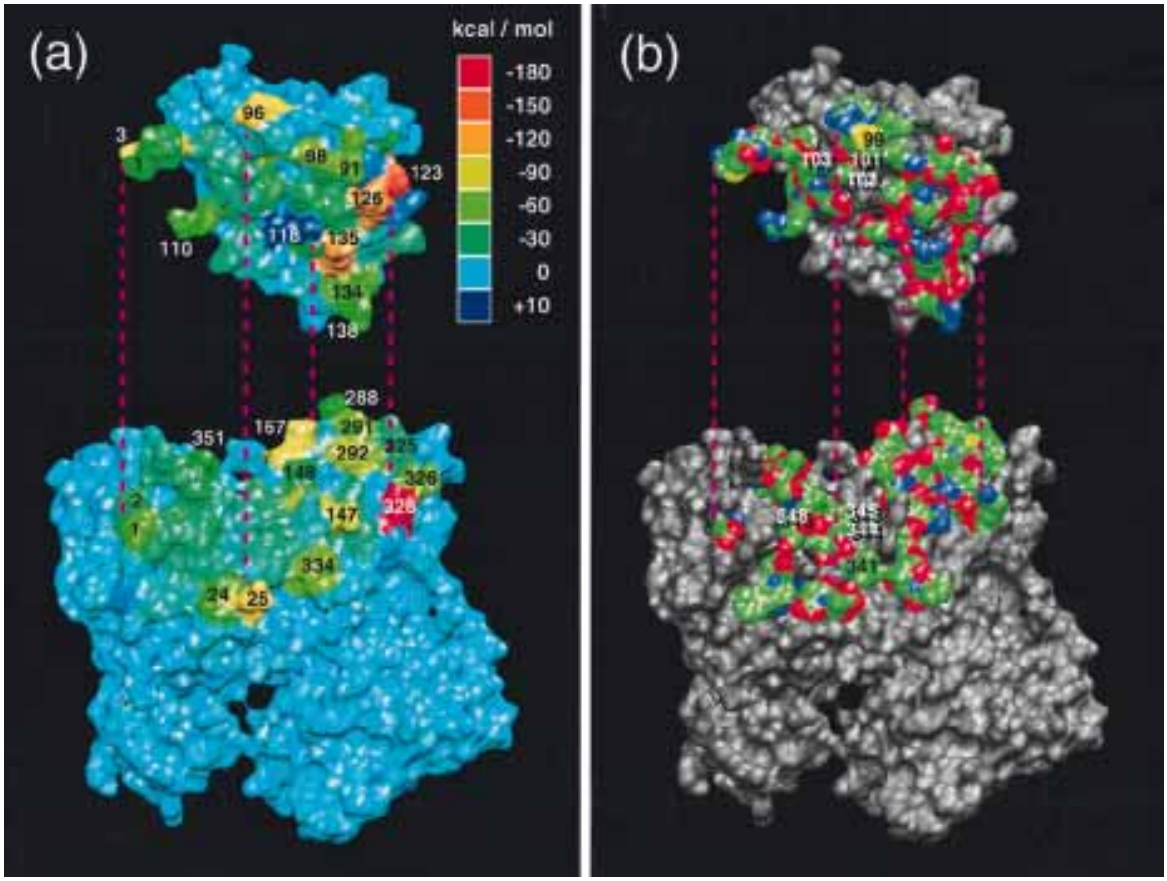

Figure 2. (a) Non-bonded interaction energies in the complex. Cofilin was rotated by 90° about the horizontal axis and translated from the binding site to expose the actin binding face. The form used for the total potential energy in the simulations discussed here is the CHARMM energy function (Brooks *et al.*, 1983), which involves two, three and four-atom interactions of covalently bonded atom chains, and non-bonded interactions between pairs of unconnected atoms. The non-bonded interaction energy between an atom i of actin and an atom j of cofilin has the form (Brooks *et al.*, 1983)

$$V_{ij} = \left\{ \underbrace{4\varepsilon_{ij}\left[\left(\frac{\sigma_{ij}}{r_{ij}}\right)^{12} - \left(\frac{\sigma_{ij}}{r_{ij}}\right)^{6}\right]}_{V_{Lennard-Jones}} + \underbrace{\left(\frac{q_i q_j}{\varepsilon r_{ij}}\right)}_{V_{Coulomb}} \right\} f_{\text{cut}}(r_{ij}), \tag{1}$$

where r_{ij} is the distance between atoms i and j and ε is the dielectric constant. The switching function $f_{\text{cut}}(r_{ij})$ (Brooks *et al.*, 1983) truncates all non-bonded interactions outside a cut-off radius (here: 12 Å), to reduce the computational cost of pairwise interactions in large systems. The partial charges q_i and the Lennard-Jones parameters (ε_{ij}, σ_{ij}) are provided in standardized form (Brooks *et al.*, 1983). The interaction energy of a given residue of actin with cofilin was determined by summing the V_{ij} over atoms i belonging to the residue and over atoms j of cofilin. Interaction energies between a given residue of cofilin with actin were computed similarly. The computed interaction energies of individual residues describe the unscreened enthalpic contributions of hydrogen bonds, salt-bridges and van der Waals contacts to the total protein-protein interaction energy. Actin's subdomains 2 and 4 were added for visualization. (b) Contact surfaces in the complex. The model of the actin-cofilin complex was analyzed with the distance functions in X-PLOR to determine the contact interface. For each amino acid a search of all atoms located within a distance of 2.5 Å was conducted. The parent amino acid residue of any found atom not belonging to the same protein was defined as making a contact. Molecular surfaces that become buried are colored: yellow (sulfur), red (oxygen), blue (nitrogen), and green (carbon).

on actin (rms deviation 1.9 Å), but induced a conformational change in cofilin (see below). The forming of the salt bridges from cofilin Arg96 and Lys98 to actin had little effect on either protein, so that both structures finally stabilized at 2 Å rms deviation from the crystal conformation.

The conformational changes observed in cofilin (Figure 3(a)) involve mainly a displacement of Ala9 (at the start of helix 1), and movements of helix 2 (residues 52 to 55) and of the 4-5 turn (residues 74 to 77). A detailed inspection of the structures revealed that the binding of cofilin's N

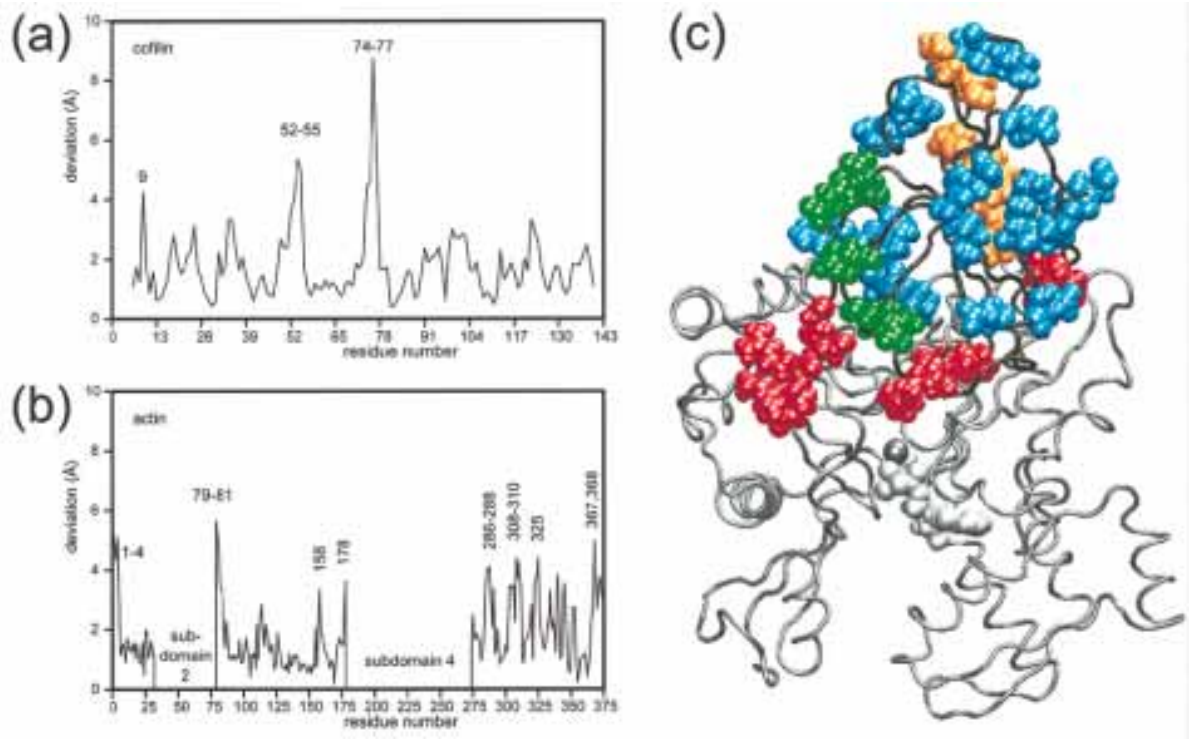

Figure 3. Deviation of the final cofilin (a) and actin (b) structures from the crystal coordinates (Fedorov *et al*., 1997; McLaughlin *et al*., 1993). The deviations in (a) and (b) were computed as a function of residue number for least-squares fitted (Kabsch, 1976) α-carbons in cofilin and actin. Actin's subdomains 2 and 4 were not part of the simulated system. (c) Comparison of the complex structure with mutagenesis results (Lappalainen *et al*., 1997). Cofilin residues that were subject to mutation (Lappalainen *et al*., 1997) are shown as colored van-der-Waals spheres; red: mutations exhibited defects in both G and F-actin binding; orange: mutations exhibited defects only in F-actin binding; blue: mutations exhibit wild-type behavior; green: mutations exhibit wild-type behavior *in vitro*, but lethal phenotype *in vivo* (Lappalainen *et al*., 1997). The cofilin backbone is shown in black tube representation, actin in grey tube representation. Actin's subdomains 2 and 4 were added for visualization. ATP (light gray) and the associated calcium ion (dark gray) are represented by van-der-Waals spheres.

terminus to actin led to a break up of a hydrogen bond in the crystal structure between the main-chain of Ala9 with the side-chain of Val8 (not shown). Instead, the Ala9 main-chain now interacted in an α-helical mode with the main-chain of Leu13, and the side-chain of Val8 formed a new hydrogen bond with the side-chain of Leu13. Thereby, Ala9 became part of helix 1. The observed movements of helix 2 and the 4-5 turn are likely due to thermal disorder, since both structure elements are solvent-exposed and distant from the actin binding face (Figure 1(c)). A test of the stereochemical quality of the simulated structure of cofilin with the program PROCHECK (Laskowski *et al*., 1993) showed that all but one amino acid exhibited backbone torsional angles in the sterically allowed range of values (data not shown). The sole offending residue was Asn76 in the tip of the flexible 4-5 turn.

The deviating actin regions (Figure 3(b)) are located, in most cases, either at the subdomain 2/4 binding face (residues 79 to 81, 158, 178, 308 to 310) or at the cofilin binding face (residues 1 to 4, 286 to 288, 325). The sole exception to this pattern are residues 367 and 368. These residues lie in a solvent-exposed region of actin's subdomain-1 that was shown to be flexible in earlier computer simulations (Wriggers & Schulten, 1997). Most of the changes observed in actin, however, can be attributed either to the truncation of subdomains 2 and 4 in the model, or to the binding of cofilin. Of special interest are interactions induced by cofilin which led to the displacement of flexible actin surface regions (residues 14, 286 to 288, 325) by 4 Å towards corresponding side-chains of cofilin.

Comparison with mutation results

The present work was well advanced when a systematic study of *in vivo* phenotypes of cofilin mutants was reported. The mapping of mutated residues onto the structure of cofilin indicated molecular surfaces that are responsible for various G and F-actin related functions (Lappalainen *et al*., 1997). These mutagenesis results furnish a stringent test of the predicted model of the G-actin-cofilin complex. Lappalainen *et al*. investigated 20 yeast cofilin mutants which involved, in most cases, alanine mutations of two or three adjacent, charged residues. Figure 3(c) maps these residues onto the

structure of the predicted actin-cofilin complex, and classifies them by the functional deficiencies caused by mutation. According to Lappalainen *et al*., mutations of cofilin residues 18, 20, 42, 43, 47, 51, 55, 56, 59, 61, 77, 79, 105, 106, 109, 110, and 130 show wild-type behavior *in vivo* and *in vitro*. Mutations involving residues 10, 11, 34, 36, and 38 exhibit wild type behavior in G and F-actin binding assays, but lethal phenotype (due to an unknown biochemical function apparently unrelated to actin binding). Mutations/deletions of residues 1-5, 96, 98, 123, and 126 inhibited both G and F-actin binding. Mutations of residues 80, 82, 134, 135, 138, inhibited F-actin binding only. Mutations involving residues 23, 24, and 26 led to aggregation of cofilin, and mutations of residues 68, 70, and 72 denatured the protein, rendering it unsuitable for biochemical assays.

As can be seen in Figure 3(c), the locations of the functional deficiencies agree well with our model of the complex. The residues which affect G-actin binding are involved in strong interactions in our model. Residues that only inhibit F-actin binding appear on a separate surface that may be part of a region of steric clash in the filament (see Discussion). Most mutations that retain wild-type phenotype are in residues distant from the proposed actin binding face. Mutated residues that produce lethal phenotype but retain normal in vitro behavior comprise yet another separate functional surface of cofilin distant from the actin binding face (Figure 3(c)), as do the residues which denature or aggregate cofilin (not shown).

Our model is also consistent with a recent mutation study of the cofilin-related maize actin depolymerization factor (MADF; Jiang *et al*., 1997). Mutation of a Tyr/Ala residue pair equivalent to cofilin's Tyr101 and Ala102 located in the hydrophobic core of the predicted cofilin-actin interface (Figure 2(b)) decreased the binding affinity of MADF to both G and F-actin. Furthermore, mutation of two tyrosine residues equivalent to cofilin's Tyr64 and Tyr67 abolishes F but not G-actin binding, which implies that at least one of the two residues plays a critical role in F-actin binding (Jiang *et al*., 1997). Tyr67, located near a region of cofilin which is predicted to bind F-actin (J.X.T., W.W. & P.A.J., unpublished results), appears to be suitable to perform such a functional role.

Competition between cofilin and GS160 for binding G-actin

The simulation studies of the cofilin-actin complex structure predict that cofilin and gelsolin segment-1 will compete for binding to actin monomers. This prediction was verified by biochemical analysis. Two types of assays compared the binding of cofilin and GS160 to monomeric actin. One set of experiments used agarose-coupled G-actin to co-precipitate binding partners. The second assay used Ni beads that precipitate histidine-tagged GS160 to examine how cofilin interfered with the binding of actin to this gelsolin construct.

Cofilin prevents the binding of gelsolin or GS160 to G-actin immobilized on agarose beads

Adding cofilin to immobilized G-actin inhibits the binding of both intact gelsolin and GS160, as shown in Figure 4 by the decreased co-sedimentation of the gelsolin constructs with actin (Figure 4(b)), their release into the supernatant fractions (Figure 4(a)), and their replacement by actin-bound cofilin. Comparison of lanes 4 to 5 and 8 to 9 shows that addition of cofilin to gelsolin-actin complexes dissociates gelsolin from actin as efficiently as adding cofilin to actin first prevents the binding of gelsolin to actin.

Cofilin displaces G-actin from histidine-tagged GS160 in a Ni-bead assay

The mutually exclusive binding of cofilin and GS160 to actin monomers was confirmed in a different assay in which free actin was added to mixtures of cofilin and histidine-tagged GS160 prior to selective sedimentation of GS160 by Ni-agarose beads (Figure 4(c)). Competition between GS160 and cofilin was assessed by the ability of cofilin to reduce the amount of G-actin co-sedimenting with GS160. In the absence of cofilin, sedimentation of GS160 co-precipitates an equimolar amount of G-actin (lane 4), leaving a smaller amount in the supernatant fraction (lane 3). Addition of increasing amounts of cofilin reduced the amount of G-actin co-sedimenting with GS160 (lanes 6 and 8) and increased the amount of actin in the supernatant (lanes 5 and 7). A quantitative comparison of the amounts of gelsolin bound to actin in the presence of increasing cofilin is shown in Figure 4(d), where the decrease in actin co-sedimenting with GS160 is accompanied by a corresponding release of actin into the supernatant fraction as increasing amounts of cofilin are added. Formation of a ternary complex containing actin, cofilin, and GS160 was not observed, as the slight amount of cofilin appearing in the pellet fraction is accounted for by non-specific sedimentation or adhesion in the absence of actin (lane 2).

Discussion

The remarkable diversity of interactions between actin and the family of small (19 to 21 kDa) proteins related to cofilin, including ADF, destrin, depactin, and actophorin suggest that subtle differences in the actin binding site of these proteins lead to large differences in actin filament stability and structure. Unlike larger proteins such as gelsolin where differential effects on actin are related to selective involvement of multiple actin binding sites, cofilin appears to engage all or part of the

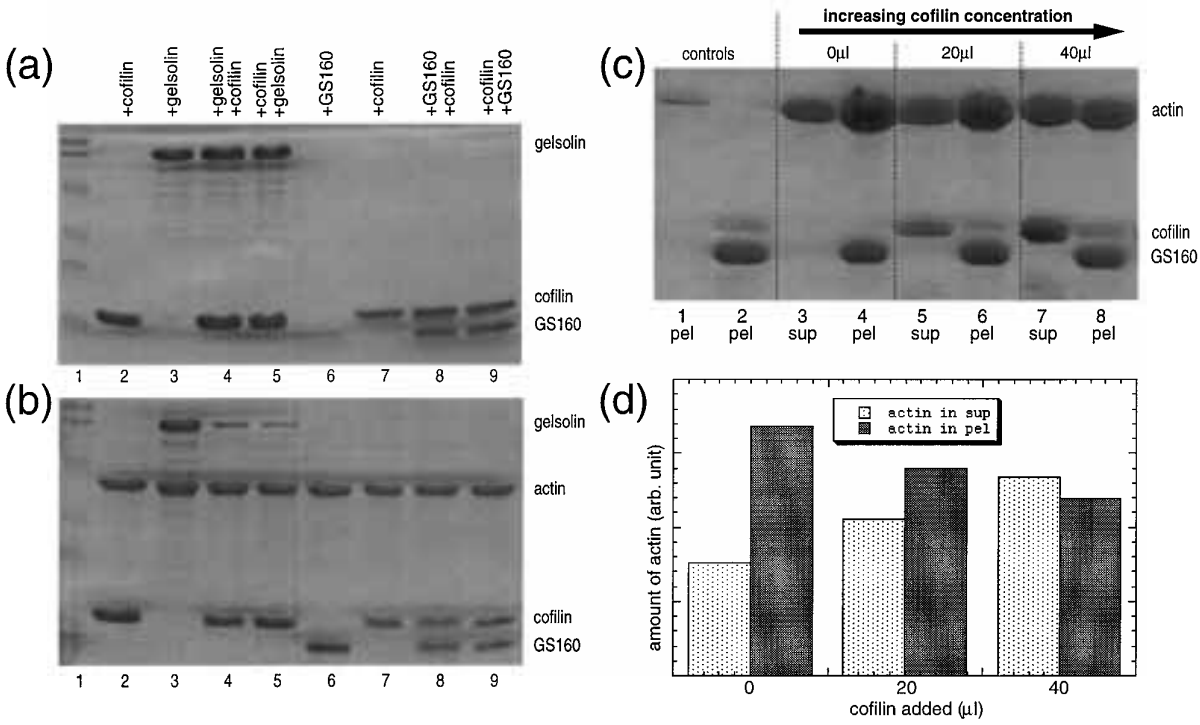

Figure 4. Competitive binding of cofilin and gelsolin to G-actin-agarose beads: Supernatants (a) and pellets (b). G-actin was immobilized on CNBr activated Sepharose 4B beads, by standard methods (Haddad *et al*., 1984; Janmey *et al*., 1986; Pope *et al*., 1991) and proteins bound to G-actin detected by SDS-PAGE analysis of pellets formed by low speed sedimentation (14,000*g*) of actin-Sepharose under conditions where the free proteins would not sediment. In order to detect competitive binding, approximately 30 µg G-actin-Sepharose beads were added to mixtures of cofilin, gelsolin, and GS160. After sedimentation, the beads were washed once in G-actin buffer solution, once in this solution plus 150 mM KCl, and again in G-actin buffer solution. The proteins bound to the beads were subjected to SDS-PAGE and detected by Coomassie blue staining. By adding SDS sample buffer and heating the samples at 97°C for a few minutes all the proteins including actin were found to be separated from the beads. Lane 2: 100 µg cofilin; lane 3: 100 µg gelsolin; lane 4: incubation with 100 µg gelsolin (30 minutes), followed by incubation with 100 µg cofilin (30 minutes); lane 5: incubation with 100 µg cofilin (30 minutes), followed by incubation with 100 µg gelsolin (30 minutes); lanes 6 to 9: same design as lanes 2 to 5, but GS160 was used instead of intact gelsolin, and reduced amounts of GS160 (20 µg) and cofilin (40 µg) were used. The final volume of each sample was 140 µl. For the assays in (a) to (c), G-actin was prepared from an acetone powder of rabbit skeletal muscle (Spudich and Watt, 1971). The non-polymerizing solution contained 2 mM Hepes buffer at pH 7.5, 0.2 mM $CaCl_2$, 0.5 mM ATP, and 0.5 mM NaN_3. Human plasma gelsolin was purified by elution from DE-52 ion exchange matrix in 30 mM NaCl, 3 mM $CaCl_2$, 25 mM Tris (pH 7.4) as described by Kurokawa *et al*.(1990), rapidly frozen in liquid nitrogen and stored at −80°C. A fragment of rat gelsolin containing amino acids 26 to 160 (GS160; Kwiatkowski *et al*., 1989) with a 6-histidine tag at the N terminus was expressed in *E. coli* and purified as described elsewhere (Fujita *et al*., 1997). Full-length recombinant cofilin was prepared by introducing an NdeI restriction enzyme site into a cDNA clone for human cofilin kindly provided by Dr Colin Casimir. The *NdeI* site was placed 3 bp prior to the initiation methionine in order to allow cloning into the *NdeI* site of pMW172 without the introduction of additional amino acid residues. The bacterial strain BL21(DE3)-PLysS was used for protein expression. The soluble bacterial extract was passed over a DE52 column in a buffer containing 10 mM Tris-HCl (pH 8.0) and 1 mM EGTA, and the flow-through, in which cofilin was present, was collected. Cofilin prepared in this manner was greater than 95% pure as judged by SDS-PAGE analysis. (c) Displacement of G-actin by cofilin from histidine-tagged GS160. Each sample contained a sufficient number of Ni beads to immobilize 20 µl of 100 µM GS160. Lane 1: 20 µM G-actin, no GS160; lane 2: 20 µl (100 µM) cofilin and 20 µl (100 µM) GS160, no G-actin. Three samples were tested in addition to the controls. Each sample contained 40 µl of 50 µM G-actin and 2 µl of 100 mM Ca^{2+}. Lanes 3 and 4: no cofilin; lanes 5 and 6: 20 µl (100 µM) cofilin; lanes 7 and 8: 40 µl (100 µM) cofilin. The final volume of each sample was 200 µl. (d) Comparison of amounts of actin cosedimenting with GS160 and remaining in the supernatant derived from the data in (c). An estimate of the amount of protein in each lane was made by scanning the Coomassie-stained gels using a standard commercial scanner and NIH Image 1.6 software (Wayne Rasband, Bethesda MD).

same binding face to sequester actin monomers, bind stably to the sides of actin filaments, induce filament bundling, and disassemble actin filaments either by accelerating subunit release or by direct severing of the filament. Some of the effects of cofilin resemble those of gelsolin and its homologs, including the ability to accelerate actin filament disassembly, rapidly reduce the viscosity of F-actin

solutions, and accelerate the polymerization of actin monomers.

The predicted cofilin-actin complex is consistent with the available structural and biochemical data. In particular, our model agrees with the actin binding face of cofilin suggested by biochemical studies (Sutoh & Mabuchi, 1986) and site-directed mutagenesis (Lappalainen *et al*., 1997; Jiang *et al*., 1997). There are only two sites where our model predicts stronger actin-cofilin interactions than indicated by Lappalainen *et al*. (1997). First, mutation of cofilin's Arg110, which in our model interacts with the main-chain of actin's Thr351, allows actin growth and filament organization in yeast as observed with wild-type cofilin. Second, mutation of the basic cluster Arg135 and Arg138, which interacts with an acidic cluster of G-actin in our model, was shown to affect only the binding of cofilin to F-actin, but not the binding of G-actin. Consistent with the mutagenesis results, the predicted complex exhibits strong interactions between the N termini of actin and cofilin, mediated by a salt bridge of cofilin Arg3 with actin Asp1. Phosphorylation of the adjacent cofilin Ser4 is known to negatively regulate cofilin's actin-depolymerization function (Agnew *et al*., 1995; Moriyama *et al*., 1996). The negatively charged phosphate may disturb the formation of the N to N-terminal salt bridge by binding to cofilin Arg3 or by repelling actin Asp1.

Cofilin binds to both G and F-actin in a 1:1 molar ratio (Nishida *et al*., 1984). Binding of cofilin to actin in the mode defined here may also account for at least some of its interactions with F-actin. While the gelsolin segment 1 itself presents intolerable steric clashes with the actin-actin bonds of F-actin, the slight differences in the cofilin/actin interface, and the drastic change in helical pitch when cofilin binds F-actin suggest that our model may be consistent with the cofilin bound F-actin structure determined by electron microscopy (McGough *et al*., 1997). One possible explanation of cofilin's filament destabilizing activity (Yonezawa *et al*., 1985) is a conformational transition from the F to the G-actin binding mode that weakens the interactions of adjacent monomers in the filament. Such a ''steric exclusion'' mechanism would require a certain similarity of the binding modes in both cases. Preliminary studies (J.X.T., W.W. & P.A.J., unpublished results) show that cofilin can be aligned to a model of F-actin in the predicted G-actin binding mode to form a structure consistent with recent electron microscopy reconstructions of cofilin-decorated filaments (McGough *et al*., 1997).

Cofilin bears structural resemblance to all six gelsolin segments (Burtnick *et al*., 1997). The finding that gelsolin fragments lacking segment-1 prevent cofilin binding to F-actin (Fujita *et al*., 1997) suggests a mode of F-actin binding analogous to that of the side binding domain (segments 2-3) of gelsolin which does not bind G-actin. Similarity between cofilin and gelsolin segments 2-3 is also supported by the finding that both cofilin and a peptide based on cofilin residues 102 to 130 compete with gelsolin segments 2-3 for binding F-actin, and by the preferential inhibition of cofilin-actin binding by a peptide derived from gelsolin segment-2 compared to its homolog in segment-1 (Van Troys *et al*., 1997). These results are not necessarily inconsistent with our model. The mutually exclusive binding of cofilin and gelsolin segments 2-3 to actin does not strictly imply that these constructs compete for the same binding site. Competition between cofilin and other F-actin binding proteins like gelsolin 2-6 (McGough *et al*., 1998) may involve the large structural change in F-actin induced by cofilin (McGough *et al*., 1997). Filament side-binding proteins that stabilize the normal helical pitch of the filament may prevent the conformational change required for cofilin to occupy the actin subunits in the altered conformation of the cofilin/actin monomer complex. Such competition between ligands without apparently sharing binding interfaces is exemplified by the inability of cofilin to bind phalloidin-actin complexes, even though the well-mapped actin contacts of phalloidin are in the actin filament interior, whereas cofilin binds exclusively to the filament surface.

In this context, the biochemical competition between cofilin and GS160 for actin monomers demonstrated here can be interpreted either as evidence for the same binding site on actin or that the binding of one protein allosterically alters the structure or access to the other binding site. Therefore, our simulation studies of the cofilin-actin interaction surface provide crucial support for the analogy between cofilin and gelsolin segment-1.

Despite the lack of sequence homology between cofilin and gelsolin, the tertiary structure of all cofilin-related proteins is similar to that of the gelsolin segments. This similarity (Hatanaka *et al*., 1996) is the structural basis of our work. The difference in sequence is sometimes used as an argument against a similar actin-binding mode between cofilin and gelsolin segment-1 (Lappalainen *et al*., 1997). However, statistical studies of sequence and structure databases demonstrate that it is not unusual for proteins of similar fold to differ in their amino acid sequence (Chothia & Lesk, 1986; Hubbard, 1997). Often, newly discovered crystal structures reveal surprising relationships that could not be imagined based on the available sequence data alone; the proposed evolutionary relationship between the motor proteins kinesin and myosin is one such example (Kull *et al*., 1997).

There are major differences between the functions of cofilin and intact gelsolin, including the inability of cofilin to cap the filament end and the inability of intact gelsolin to form stable complexes with the side of actin filaments. It is not clear whether these functional differences correspond to small structural modulations of the proposed actin-binding mode or whether they correspond to several distinct binding modes. Low-resolution density maps from electron microscopy do not provide enough detail to determine the subunit orientation

in cofilin or gelsolin-decorated F-actin (McGough *et al*., 1997). A hybrid modeling approach including atomic-resolution force-fields, low-resolution density maps, and other available structural constraints may identify the sites at which gelsolin and cofilin contact actin subunits, and reveal whether these proteins exert their effects on actin by similar and competing mechanisms, or whether they achieve partially overlapping functions by distinct and potentially synergistic strategies.

The atomic coordinates of the predicted complex are available by FTP. E-mail: wriggers@ucsd.edu

Acknowledgments

We thank Steven Almo, Hideki Hatanaka and Paul McLaughlin for the coordinates of cofilin, destrin, and the actin-gelsolin segment-1 complex. We thank Phil Allen, David Kwiatkowski, Amy McGough and Lisa Flanagan for valuable suggestions and advice and Albert Lee for technical assistance. W.W. was supported in part by NIH-grants to Klaus Schulten at UIUC and to J. Andrew McCammon at UCSD, and by the LJIS Interdisciplinary Training Program/Burroughs Wellcome Fund. J.X.T., T.A., P.M, and P.A.J. acknowledge support by NIH grants K08 HL03235 and AR38910.

References

Agnew, B. J., Minamide, L. S. & Bamburg, J. R. (1995). Reactivation of phosphorylated actin-depolymerizing factor and identification of the regulatory site. *J. Biol. Chem.* **270**, 17582–17587.

Aizawa, H., Sutoh, K. & Yahara, I. (1996). Overexpression of cofilin stimulates bundling of actin filaments, membrane ruffling, and cell movement in *Dictyostelium*. *J. Cell Biol.* **132**, 335–344.

Anderson, D. E., Becktel, W. & Dahlquist, F. (1990). pH-Induced denaturation of proteins: a single salt-bridge contributes 3–5 kcal/mol to the free energy of folding of T4 lysozyme. *Biochemistry,* **29**, 2403–2408.

Babcock, M. S., Pednault, E. & Olson, W. (1994). Nucleic acid structure analysis. *J. Mol. Biol.* **237**, 125–156.

Balaeff, A., Churchill, M. E. A. & Schulten, K. (1998). Structure prediction of a complex between the chromosomal protein HMG-D and DNA. *Proteins: Struct. Funct. Genet.* **30**, 113–135.

Brooks, B. R., Bruccoleri, R. E., Olafson, B. D., States, D. J., Swaminathan, S. & Karplus, M. (1983). CHARMM: A program for macromolecular energy, minimization, and dynamics calculations. *J. Comp. Chem.* **4**, 187–217.

Brünger, A. T. (1992). *X-PLOR, Version 3. 1: A System for X-ray Crystallography and NMR*, Yale University Press, New Haven.

Burtnick, L. D., Koepf, E. K., Grimes, J., Jones, E. Y., Stuart, D. I., McLaughlin, P. J. & Robinson, R. C. (1997). The crystal structure of plasma gelsolin: Implications for actin severing, capping, and nucleation. *Cell,* **90**, 661–670.

Carlier, M. F., Laurent, V., Santolini, J., Melki, R., Didry, D., Xia, G. X., Hong, Y., Chua, N. H. & Pantaloni, D. (1997). Actin depolymerizing factor (ADF/cofilin) enhances the rate of filament turnover: implication in actin-based motility. *J. Cell Biol.* **136**, 1307–1322.

Chasles, M. (1830). Note sur les propriétés générales du système de deux corps semblables entre'eus et placés d'une manière quelconque dans l'espace; et sur la deplacement fini ou infinement petit d'un corps solide libre. *Férusac, Bull. Sci. Math.* **14**, 321–326.

Chothia, C. & Lesk, A. M. (1986). The relation between the divergence of sequence and structure in proteins. *EMBO J.* **5**, 823–826.

Clackson, T. & Wells, J. (1995). A hot-spot of binding energy in a hormone-receptor interface. *Science,* **267**, 383–386.

Fedorov, A., Lappalainen, P., Fedorov, E. V., Drubin, D. G. & Almo, S. C. (1997). Structure determination of yeast cofilin. *Nature Struct. Biol.* **4**, 366–369.

Fujita, H., Allen, P. G., Janmey, P. A., Azuma, T., Kwiatkowski, D. J., Stossel, T. P., Furuuchi, K. & Kuzumaki, N. (1997). Characterization of gelsolin truncates that inhibit actin depolymerization by severing activity of gelsolin and cofilin. *Eur. J. Biochem.* **248**, 834–839.

Garnier, J., Osguthorpe, D. & Robson, B. (1978). Analysis of the accuracy and implications of simple methods for predicting the secondary structure of globular proteins. *J. Mol. Biol.* **120**, 97–120.

Goldstein, H. (1980). *Classical Mechanics*, Addison-Wesley, Reading, Mass.

Haddad, J. G., Kowalski, M. A. & Sanger, J. W. (1984). Actin affinity chromatography in the purification of human, avian and other mammalian plasma proteins binding vitamin D and its metabolites (Gc globulins). *Biochem. J.* **218**, 805–810.

Hatanaka, H., Ogura, K., Moriyama, K., Ichikawa, S., Yahara, I. & Inagaki, F. (1996). Tertiary structure of destrin and structural similarity between two actin-regulating protein families. *Cell,* **85**, 1047–1055.

Holley, L. H. & Karplus, M. (1989). Protein secondary structure prediction with a neural network. *Proc. Natl Acad. Sci. USA,* **86**, 152–156.

Hubbard, T. (1997). New horizons in sequence analysis. *Curr. Opin. Struct. Biol.* **7**, 190–193.

Humphrey, W. F., Dalke, A. & Schulten, K. (1996). VMD – visual molecular dynamics. *J. Mol. Graphics,* **14**, 33–38.

Israelachvili, J. N. (1992). *Intermolecular and Surface Forces*, Academic Press, London.

Janmey, P. A., Stossel, T. P. & Lind, S. E. (1986). Sequential binding of actin monomers to plasma gelsolin and its inhibition by vitamin D-binding protein. *Biochem. Biophys. Res. Commun.* **136**, 72–79.

Jiang, C. J., Weeds, A. G., Khan, S. & Hussey, P. J. (1997). F-actin and G-actin binding are uncoupled by mutation of conserved tyrosine residues in maize actin depolymerizing factor (zmadf). *Proc. Natl Acad. Sci. USA,* **94**, 9973–9978.

Kabsch, W. (1976). A solution for the best rotation to relate two sets of vectors. *Acta Crystallog. sect. A,* **32**, 922–923.

Kabsch, W., Mannherz, H. G., Suck, D., Pai, E. F. & Holmes, K. C. (1990). Atomic structure of the actin: DNase I complex. *Nature,* **347**, 37–44.

King, G., Lee, F. & Warshel, A. (1991). Microscopic simulations of macroscopic dielectric constants of proteins. *J. Chem. Phys.* **95**, 4366–4377.

Kull, F. J., Sablin, E. P., Lau, R., Fletterick, R. J. & Vale, R. D. (1997). Crystal structure of the kinesin motor

domain reveals a structural similarity to myosin. *Nature,* **380**, 550–555.
Kurokawa, H., Fujii, W., Ohmi, K., Sakurai, T. & Nonomura, Y. (1990). Simple and rapid purification of brevin. *Biochem. Biophys. Res. Commun.* **168**, 451–457.
Kwiatkowski, D. J., Janmey, P. A. & Yin, H. L. (1989). Identification of critical functional and regulatory domains in gelsolin. *J. Cell Biol.* **108**, 1717–1726.
Lappalainen, P., Fedorov, E. V., Fedorov, A., Almo, S. C. & Drubin, D. G. (1997). Essential functions and actin-binding surfaces of yeast cofilin revealed by systematic mutagenesis. *EMBO J.* **16**, 5520–5530.
Laskowski, R. A., MacArthur, M. W., Moss, D. S. & Thornton, J. M. (1993). PROCHECK: a program to check the stereochemical quality of protein structures. *J. Appl. Crystallog.* **26**, 283–291.
Leonard, S. A., Gittis, A. G., Petrella, E. C., Pollard, T. D. & Lattman, E. A. (1997). Crystal structure of the actin-binding protein actophorin from Acanthamoeba. *Nature Struct. Biol.* **4**, 369–373.
Mabuchi, I. (1983). An actin-depolymerizing protein (depactin) from starfish oocytes: properties and interaction with actin. *J. Cell Biol.* **97**, 1612–1621.
Maciver, S. K., Wachsstock, D. H., Schwarz, W. H. & Pollard, T. D. (1991). The actin filament severing protein actophorin promotes the formation of rigid bundles of actin filaments crosslinked with alpha-actinin. *J. Cell Biol.* **115**, 1621–1628.
McGough, A., Pope, B., Chiu, W. & Weeds, A. (1997). Cofilin changes the twist of F-actin – implications for actin filament dynamics and cellular function. *J. Cell Biol.* **138**, 771–781.
McGough, A., Chiu, W. & Way, M. (1998). Determination of the gelsolin binding site on F-actin: implications for severing and capping. *Biophys. J.* **74**, 764–772.
McLaughlin, P. J., Gooch, J. T., Mannherz, H. G. & Weeds, A. G. (1993). Structure of gelsolin segment 1-actin complex and the mechanism of filament severing. *Nature,* **364**, 685–692.
Molecular Simulations Inc. (1994). Quanta 4.0, Burlington, Massachusetts.
Moon, A. L., Janmey, P. A., Louie, K. A. & Drubin, D. G. (1993). Cofilin is an essential component of the yeast cortical cytoskeleton. *J. Cell Biol.* **120**, 421–435.
Morgan, T. E., Lockerbie, R. O., Minamide, L. S., Browning, M. D. & Bamburg, J. R. (1993). Isolation and characterization of a regulated form of actin depolymerizing factor. *J. Cell Biol.* **122**, 623–633.
Moriyama, K., Yonezawa, N., Sakai, H., Yahara, I. & Nishida, E. (1992). Mutational analysis of an actin-binding site of cofilin and characterization of chimeric proteins between cofilin and destrin. *J. Biol. Chem.* **267**, 7240–7244.
Moriyama, K., Iida, K. & Yahara, I. (1996). Phosphorylation of Ser3 of cofilin regulates its essential function on actin. *Genes Cells,* **1**, 73–86.
Nagaoka, R., Kusano, K., Abe, H. & Obinata, T. (1995). Effects of cofilin on actin filamentous structures in cultured muscle cells. Intracellular regulation of cofilin action. *J. Cell Sci.* **108**, 581–593.
Nebl, G., Meuer, S. C. & Samstag, Y. (1996). Dephosphorylation of serine 3 regulates nuclear translocation of cofilin. *J. Biol. Chem.* **271**, 26276–26280.
Nishida, E., Maekawa, S. & Sakai, H. (1984). Cofilin, a protein in porcine brain that binds to actin filaments and inhibits their interactions with myosin and tropomyosin. *Biochemistry,* **23**, 5307–5313.
Nishida, E., Muneyuki, E., Maekawa, S., Ohta, Y. & Sakai, H. (1985). An actin-depolymerizing protein (destrin) from porcine kidney. Its action on F-actin containing or lacking tropomyosin. *Biochemistry,* **24**, 6624–6630.
Nishida, E., Iida, K., Yonezawa, N., Koyasu, S., Yahara, I. & Sakai, H. (1987). Cofilin is a component of intranuclear and cytoplasmic actin rods induced in cultured cells. *Proc. Natl Acad. Sci. USA,* **84**, 5262–5266.
Ohta, Y., Nishida, E., Sakai, H. & Miyamoto, E. (1989). Dephosphorylation of cofilin accompanies heat shock-induced nuclear accumulation of cofilin. *J. Biol. Chem.* **264**, 16143–16148.
Pope, B., Way, M. & Weeds, A. G. (1991). Two of the three actin-binding domains of gelsolin bind to the same subdomain of actin. Implications of capping and severing mechanisms. *FEBS Letters,* **280**, 70–74.
Smith, P. E., Brunne, R. M., Mark, A. E. & van Gunsteren, W. F. (1993). Dielectric properties of trypsin inhibitor and lysozyme calculated from molecular dynamics simulations. *J. Phys. Chem.* **97**, 2009–2014.
Spudich, J. & Watt, S. (1971). The regulation of rabbit skeletal muscle contraction. I. Biochemical studies of the interaction of the tropomyosin-troponin complex with actin and the proteolytic fragments of myosin. *J. Biol. Chem.* **246**, 4866–4871.
Strynadka, N. C. J., Eisenstein, M., Katchalski-Katzir, E., Shoichet, B. K., Kuntz, I. D., Abagyan, R., Totrov, M., Janin, J., Cherfils, J., Zimmerman, F., Olson, A., Duncan, B., Rao, M., Jackson, R., Sternberg, M. & James, M. N. G. (1996). Molecular docking programs successfully predict the binding of a β-lactamase inhibitory protein to TEM-1 β-lactamase. *Nature Struct. Biol.* **3**, 233–239.
Sutoh, K. & Mabuchi, I. (1986). Improved method for mapping the binding site of an actin-binding protein in the actin sequence. Use of a site-directed antibody against the N-terminal region of actin as a probe of its N-terminus. *Biochemistry,* **25**, 6186–6192.
Van Troys, M., Dewitte, D., Vershelde, J.-L., Goethals, M., Vandekerckhove, J. & Ampe, C. (1997). Analogous F-actin binding by cofilin and gelsolin segment 2 substantiates their structural relationship. *J. Biol. Chem.* **272**, 32750–32758.
Wriggers, W. & Schulten, K. (1997). Stability and dynamics of G-actin: back door water diffusion and behavior of a subdomain 3/4 loop. *Biophys. J.* **73**, 624–639.
Wriggers, W. & Schulten, K. (1998). Nucleotide-dependent movements of the kinesin motor domain predicted by simulated annealing. *Biophys J.* **75**, 646–661.
Yahara, I., Aizawa, H., Moriyama, K., Iida, K., Yonezawa, N., Nishida, E., Hatanaka, H. & Inagaki, F. (1996). A role of cofilin/destrin in reorganization of actin cytoskeleton in response to stresses and cell stimuli. *Cell Struct. Funct.* **21**, 421–424.
Yonezawa, N., Nishida, E. & Sakai, H. (1985). pH Control of actin polymerization by cofilin. *J. Biol. Chem.* **260**, 14410–14412.
Yonezawa, N., Nishida, E., Maekawa, S. & Sakai, H. (1988). Studies on the interaction between actin and

cofilin purified by a new method. *Biochem. J.* **251**, 121–127.
Yonezawa, N., Nishida, E., Ohba, M., Seki, M., Kumagai, H. & Sakai, H. (1989). An actin-interacting heptapeptide in the cofilin sequence. *Eur. J. Biochem.* **183**, 235–238.
Yonezawa, N., Homma, Y., Yahara, I., Sakai, H. & Nishida, E. (1991a). A short sequence responsible for both phosphoinositide binding and actin binding activities of cofilin. *J. Biol. Chem.* **266**, 17218–17221.
Yonezawa, N., Nishida, E., Iida, K., Kumagai, H., Yahara, I. & Sakai, H. (1991b). Inhibition of actin polymerization by a synthetic dodecapeptide patterned on the sequence around the actin-binding site of cofilin. *J. Biol. Chem.* **266**, 10485–10489.

Edited by J. Karn

(Received 6 April 1998; received in revised form 3 July 1998; accepted 9 July 1998)